PCCP

RSC Publishing

COMMUNICATION

View Article Online
View Journal | View Issue



Cite this: *Phys. Chem. Chem. Phys.*, 2013, **15**, 4892

Received 20th February 2013,
Accepted 22nd February 2013

DOI: 10.1039/c3cp50767j

www.rsc.org/pccp

# High power enzymatic biofuel cell based on naphthoquinone-mediated oxidation of glucose by glucose oxidase in a carbon nanotube 3D matrix†

Bertrand Reuillard, Alan Le Goff, Charles Agnès, Michael Holzinger, Abdelkader Zebda, Chantal Gondran, Kamal Elouarzaki and Serge Cosnier*

**We report the design of a novel glucose/$O_2$ biofuel cell (GBFC) integrating carbon nanotube-based 3D bioelectrodes and using naphthoquinone-mediated oxidation of glucose by glucose oxidase and direct oxygen reduction by laccase. The GBFCs exhibit high open circuit voltages of 0.76 V, high current densities of 4.47 mA $cm^{-2}$, and maximum power output of 1.54 mW $cm^{-2}$, 1.92 mW $mL^{-1}$ and 2.67 mW $g^{-1}$. The GBFC is able to constantly deliver 0.56 mW h $cm^{-2}$ under discharge at 0.5 V, showing among the best *in vitro* performances for a GBFC. Using a charge pump, the GBFC finally powered a Light Emitting Diode (LED), demonstrating its ability to amplify micro watts to power mW-demanding electronic devices.**

## Introduction

Among new sources of sustainable and renewable energy, the concept of biofuel cells appeared four decades ago that convert chemical energy into electrical energy by the catalytic reaction of enzymes or microorganisms. A vast majority of these biofuel cells produces electrical power from the electro-enzymatic degradation of glucose and oxygen, two substrates present in plants and physiological fluids such as blood or extracellular fluid.[1–4] Therefore, considerable attention has recently been paid to the possibility of implantation of biofuel cells in the human body. We and others recently demonstrated the possibility to harvest energy from biofuel cells implanted in rats,[5] insects,[6] clams,[7] snails[8] or lobsters.[9] However, the major obstacle for implantation into mammals lies in the weak power of biofuel cells. In addition, the concentration of glucose and $O_2$ is low in the human body which makes the problem of energy conversion even more critical since the biofuel cells power is proportional to the concentration of these compounds.

In recent years, carbon nanotubes (CNTs) have become a privileged electrode material in GBFC, not only for their high specific surface and high conductivity but also for their Direct Electron Transfer (DET) properties towards many types of redox enzymes.[10] The most powerful glucose biofuel cells (GBFCs) have taken advantage of the properties of CNT networks to maximize the density of wired enzymes per surface or volume unit and to optimize electron transfer between active sites of enzymes and the electrode surface. For instance, Mano and co-workers designed a high power GBFC based on mediated electron transfer (MET) using osmium-based redox hydrogels combined with a Multi-Walled CNT (MWCNT)-based electrode for indirect enzyme wiring.[11] Recently, we reported the possibility of creating enzyme electrodes by compression of enzyme–MWCNT mixtures. Moreover, we demonstrated the efficient wiring of enzymes in a MWCNT matrix, achieving the design of a GBFC with an open-circuit voltage of 0.95 V and a maximum power output of 1.25 mW $cm^{-2}$ in 0.05 mol $L^{-1}$ glucose solution.[12] The latter involved DET between MWCNT matrices and glucose oxidase (GOx) at the anode and laccase at the cathode that catalyzed the oxidation of glucose and the reduction of $O_2$ in water, respectively. Although glucose concentration was markedly higher than that of $O_2$, the GBFC performance was limited by the GOx-based anode. The electrical wiring of laccase was indeed more efficient than that of GOx, which displays a prosthetic group deeply embedded within the protein shell.

With the aim of improving the GBFC performance, we report here the combination of DET and MET for the electrical wiring of GOx. Thanks to the low solubility of naphthoquinone (NQ) in water and its redox potential $E_{1/2} = -0.17$ V compatible with that of the FAD $E_{1/2} = -0.48$ V, NQ was integrated in the MWCNT matrix for increasing the density of wired enzymes per volume unit. By combining DET and MET in the MWCNT matrix, we show the advantage of using redox mediators to achieve high catalytic current densities. The optimized NQ-MWCNT-GOx matrix configuration was associated with a laccase-based biocathode and the performances of the resulting GBFC were investigated in terms of power output and stability under constant discharge.

*UJF-Grenoble 1, CNRS, Département de Chimie Moléculaire, UMR-5250, ICMG FR-2607, BP-53, 38041 Grenoble Cedex 9, France. E-mail: serge.cosnier@ujf-grenoble.fr; Fax: +33 04 56 52 08 03; Tel: +33 04 56 52 08 10*

† Electronic supplementary information (ESI) available: Fig. S1, S2 and video. See DOI: 10.1039/c3cp50767j

## Experimental part

### Methods and instrumentation

All reagents and enzymes were purchased from Aldrich. MWCNTs were purchased from Nanocyl (>95% purity, 10 nm diameter). The electrochemical characterization of each electrode was carried out in a three-electrode electrochemical cell using a Biologic potentiostat. A platinum grid was used as the counter electrode and a saturated calomel electrode (SCE) served as reference electrode. All potentials are referred to the SCE reference electrode. For the electrochemical characterization of the biofuel cell, the anode was set as working electrode while the cathode was plugged as counter-reference electrode.

All experiments were conducted at 25 or 40 °C in 0.2 mol $L^{-1}$ phosphate buffer solution (PBS, pH 7) as the supporting electrolyte.

The morphology of the MWCNT electrodes was investigated by SEM using an ULTRA 55 FESEM based on the GEMENI FESEM column with beam booster (Nanotechnology Systems Division, Carl Zeiss NTS GmbH, Germany) and tungsten gun.

### Preparation of MWCNT electrodes

**Preparation of the bioanode.** MWCNT pellets were obtained by soft grinding of a mixture of 100 μL of water, 5 mg of *p*-naphthoquinone, 15 mg of GOx from *Aspergillus niger* (139 U $mg^{-1}$), 10 mg of catalase from bovine liver (16 000 U $mg^{-1}$) and 35 mg of MWCNTs. Catalase was used in combination with GOx in order to catalyze both the decomposition of hydrogen peroxide and the removal of oxygen at the bioanode. The homogenous paste is then compressed in a hydraulic press to obtain a pellet with 5 mm diameter and 4 mm thickness, leading to a bioelectrode volume of 0.08 mL. A copper wire is connected to one side of the pellet by a conductive adhesive. Silicone is added to cover the sides, electrical wires and conductive adhesive, leaving one side of the pellet that corresponds to the electrochemical surface of the electrode with a geometrical surface of 0.2 $cm^2$. After incubation of the electrode in PBS for 5 min, 50 μL of a mixture of 0.1 mol $L^{-1}$ pyrrole and 0.1 mol $L^{-1}$ polystyrene sulfonate (PSS) was drop-casted onto the electrode surface. Electropolymerisation was then performed at 0.9 V for 10 minutes, affording a polypyrrole–PSS (PPy–PSS) polymer film on the electrode surface (Fig. S1, ESI†).

**Preparation of the biocathode.** A similar procedure was employed using 15 mg of laccase from *Trametes versicolor* (210 U $mg^{-1}$). A sheet of Nafion (Alpha Aesar, NRE-212, 0.05 mm thick sheet) was deposited in order to cover the remaining electrode surface.

**LED supply experiments.** The GBFC was connected to a low input voltage boost converter (BQ25504, Texas instruments, Dallas, Texas, USA). The global efficiency was estimated at 80% in the conditions of the GBFC operation (input voltage: 0.3 V to 0.6 V, input current: 10 to 100 μA, output voltage: 3 V). The power management principle relies on a capacitor charging through the boost voltage converter. As soon as the capacitor is fully charged, the stored power is released. Charging–discharging cycles are repeated as long as the LED is connected to the GBFC. The consumption of the 0.1 ms LED flash was estimated to 1.13 mW.

## Results and discussion

### GOx/NQ/catalase MWCNT bioanode

Fabrication of the bioelectrodes follows a previously described procedure.[12,13] The homogeneous paste containing MWCNTs, enzymes and NQ is compressed to obtain a cylindrical 3D structure in which the biocatalyst and the mediator are randomly entrapped. Silicone was used to insulate and seal the sides of the MWCNT pellet. The remaining electroactive side was covered by an electropolymerized PPy–PSS membrane. A PPy–PSS membrane was chosen because it allows efficient diffusion of glucose into the MWCNT matrix, unlike a conventional Nafion membrane. Furthermore, it prevents any breaking or swelling of the electrode in contact with the electrolyte. Fig. S1 (ESI†) shows the SEM image of a MWCNT electrode before and after electrodeposition of the PPy–PSS film. SEM image from Fig. S1B (ESI†) underlines the homogeneous coverage of the surface of the MWCNT electrode with a thin polymer layer.

Cyclic voltammetry (CV) experiments were performed to address the electrocatalytic properties of the bioelectrode towards oxidation of glucose (Fig. 1). CV scans were recorded at low scan rates (0.2 mV $s^{-1}$) to subtract the important contribution of capacitive current induced by the large electroactive area of the MWCNT network.

In the absence of glucose, a reversible system is observed at $E_{1/2} = -0.46$ V (*vs.* SCE, $\Delta E = 75$ mV), corresponding to the FAD redox activity (dashed line, Fig. 1). This redox behaviour clearly confirms the immobilization of GOx in the MWCNT matrix. A large $\Delta E$ (300 mV) of the NQ redox couple as well as the presence of two overlapping reversible systems seems to indicate inhomogeneous diffusion gradient at the porous electrode surface.[14] This may also reflect more or less hydrophobic microenvironments of the entrapped NQ.

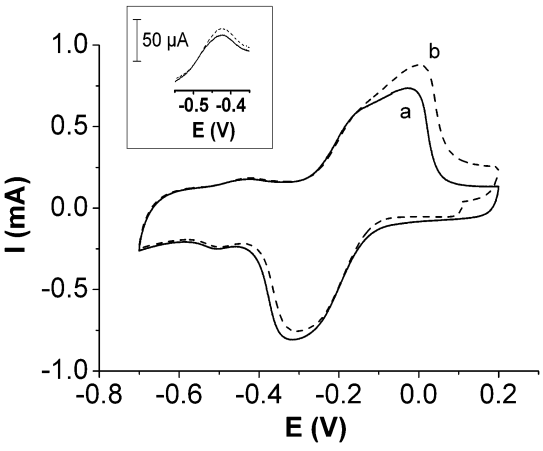


**Fig. 1** Cyclic voltammetry of the GOx/NQ/catalase MWCNT bioanode (a) without and (b) with glucose (0.15 mol $L^{-1}$) under argon. (Inset) Focus on the anodic peaks related to the direct electron transfer process with the immobilized GOx ($v$ = 0.2 mV $s^{-1}$, 0.2 mol $L^{-1}$ PBS, pH 7, 40 °C).

In the presence of glucose, both redox systems exhibit an increase in the anodic wave intensity combined with a decrease in current intensity of the corresponding cathodic peaks (Fig. 1 dashed line (b)). This electrocatalytic behaviour confirms both a direct and a mediated electron transfer at the FAD and NQ signal respectively.

The comparison of the catalytic current intensities, 0.14 mA at 0 V for the MET-based on NQ and 0.01 mA at −0.4 V for the DET to the prosthetic FAD group of GOx, clearly shows that MET provides 14-times higher catalytic activity. Although the MET process, by definition, induces a decrease in output voltage and hence in the biofuel cell power, the latter seems more interesting than the less efficient DET between FAD-GOx and MWCNTs. As expected, NQ is involved in the MET of glucose oxidation but could also thus connect to the electrode, GOx proteins wired locally by nanotubes but isolated in the matrix. However, the presence of high background currents on cyclic voltammograms prevents their use to analyze the catalytic efficiency. Therefore chronoamperometry at increasing glucose concentrations was performed to probe the electrocatalytic activity towards glucose oxidation *via* MET using NQ (Fig. 2, Fig. S2, ESI†). An apparent Michaelis–Menten dependence was derived from these experiments. For all experiments, high apparent Michaelis constant $K_m^{app}$ values ($\cong$60 mM) were determined that unambiguously arise from the slow diffusion of substrate into the 3D bioelectrode. A similar behaviour was already reported for enzymatic studies of tyrosinases immobilised in equivalent MWCNT matrices.[13]

Chronoamperometric measurements were performed with different amounts of NQ: 0, 1, 2.5 and 5 mg (inset, Fig. 2). From these experiments, the maximum current $I_{max}$ recorded at high glucose concentration is quasi-proportional to the amount of NQ incorporated into the bioelectrode.

The intercept, corresponding to the absence of NQ in the electrode, corresponds to the contribution of DET to the whole catalytic current. These results show that the presence of NQ as redox mediator in the bioelectrode increases the catalytic current values at 0.3 V by a factor 7. This underlines the essential role of NQ involved in a combined synergetic effect of MET and DET.

To further characterize the bioelectrode, the activity of the entrapped enzymes was estimated by chronoamperometry from the time-dependent increase in $H_2O_2$ concentration at saturating glucose conditions using a platinum electrode at the vicinity of the bioelectrode.[15] An identical experiment was carried out with GOx (2 μg, 139 U mg$^{-1}$) free in solution. By comparison of the rates of $H_2O_2$ production, the bioelectrode activity was estimated: 488.5 mU or 2492 mU cm$^{-2}$. Taking as assumption that the specific activity of the immobilized enzyme is equal to that in solution, this activity corresponds to the immobilization of 3.51 μg of GOx. Taking into account that one GOx molecule occupies an area of 56 nm$^2$, a compact one molecular layer of enzyme corresponds to a coverage of $3 \times 10^{-12}$ mol cm$^{-2}$ or 0.48 μg cm$^{-2}$. As a consequence, the immobilized amount of enzymatically active GOx may be estimated to 37 equivalent GOx monolayers, illustrating the porosity and roughness of the MWCNT/enzymes matrix.

From chronoamperometric experiments, a maximum current density of 3 mA cm$^{-2}$ was recorded that provides an electroenzymatic activity of 930 mU cm$^{-2}$ for the electrically wired GOx. Assuming that the immobilized enzyme fully retains its specific activity, a compact enzyme monolayer has an activity of 66.7 mU cm$^{-2}$. The electroactivity of the bioelectrode is therefore equivalent to 14 monolayers of GOx. Taking into account that we have a mixture of enzyme and nanotubes and the specific activity of the immobilized enzyme is overvalued, this result shows that the electrocatalysis occurs at the surface of the bioelectrode but also in the MWCNT matrix.

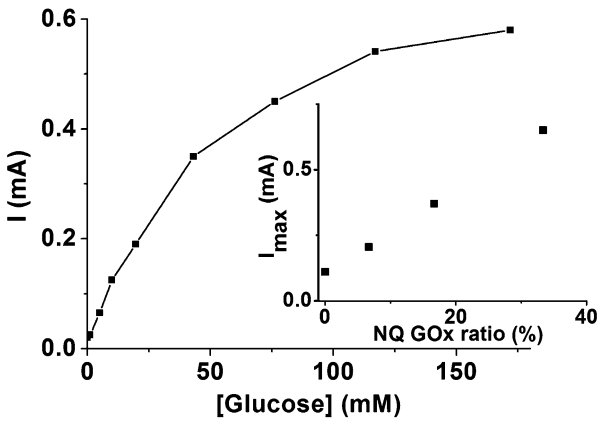


**Fig. 2** Plot of the current towards glucose concentrations for a GOx/NQ/catalase bioanode with 5 mg NQ. (Inset) Plot of the maximum current intensity towards the w/w NQ/GOx ratio.

### Laccase MWCNT biocathode

Similarly to the PPy–PSS membrane for the bioanode, the Nafion film ensures long-term stability of the 3D bioelectrode while allowing diffusion of oxygen into the MWCNT matrix.

The direct wiring of laccase in the MWCNT matrix was previously investigated by polarization curves and chronoamperometry.[12] Here we fully characterized the DET for laccase wired to the MWCNT matrix by CV experiments. CV was performed at low scan rates (0.2 mV s$^{-1}$) in the absence and presence of oxygen (Fig. 3A). In the presence of oxygen, a

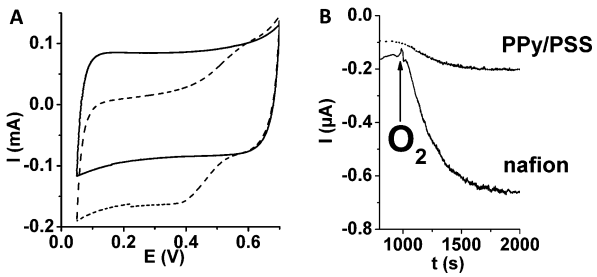


**Fig. 3** A: Cyclic voltammetry of the biocathode under argon (full line) or oxygen (dash line) saturated solution at $v$ = 0.2 mV s$^{-1}$ (0.2 mol L$^{-1}$ PBS, pH 5.5, RT); B: chronoamperometric measurement at $E$ = 0.3 V (*vs.* SCE) before and after bubbling oxygen into the electrolyte for a biocathode with a Nafion and PPy–PSS membrane. (0.2 mol L$^{-1}$ PBS, pH 7, 25 °C).

 

catalytic current for oxygen reduction is observed starting at $E$ = 0.55 V (*vs.* SCE), close to the redox potential of laccase ($E$ = 0.58 V *vs.* SCE) and stabilizing at 0.17 mA. Open-circuit potential (OCP) of 0.58 V was measured at pH 7.

In chronoamperometric measurements, we compared the important role of the chosen membrane in the catalytic current. Purging the solution with oxygen triggers an increase in intensity of the cathodic current that rapidly stabilizes at $I = -0.65$ mA and $-0.16$ mA for the biocathode respectively based on a Nafion and a PPy–PSS membrane (Fig. 3B).

### Characterization of the glucose/$O_2$ biofuel cell

Bioanode and biocathode were connected and investigated in PBS buffer (pH 7) without adding any supplementary membrane. It is well known that the optimum pH for laccase is close to 5.5 while GOx shows optimum pH at 7. We realized all the experiments at pH 7 to approach the physiological pH and obtain higher GBFC performances. Power curves were plotted from the polarization curves (Fig. 4B), which were recorded by successive one-minute discharges at constant voltages to remove the contribution of the capacitive current. Performances were registered at pH 7, in the presence of 50 mM glucose, under air and oxygen saturating conditions. Under oxygen, the GBFC exhibits maximum OCV and maximum power output values of 0.76 V and 1.54 mW cm$^{-2}$ (at 0.4 V), respectively. OCV values are in good agreement with each OCP determined for the biocathode (0.58 V) and the bioanode ($-0.20$ V). Under air, the maximum power density reached 1.1 mW cm$^{-2}$ while the OCV slightly decreased from 0.76 to 0.69 V.

To further assess the stability of the GBFC under constant discharge, the evolution of the current discharge at 0.6 V as a function of time was recorded under air and oxygen (Fig. 4C). In the early part of the long-term discharge, the high current density is due to both the high capacitive current of the CNT matrix and non-catalytic reduction and oxidation of entrapped redox molecules. Then a steady-state current of 0.6 mA cm$^{-2}$ is reached, arising from the catalytic reduction of oxygen at the biocathode and catalytic oxidation of glucose at the bioanode. Bubbling oxygen into the solution triggers the increase of current discharge from 0.6 to 1.5 mA cm$^{-2}$, demonstrating that oxygen concentration limits the biocathode performances and, by extent, the GBFC power output. This underlines the fact that the important electrocatalytic performance increase brought by the additional presence of NQ at the bioanode is limited by the biocathode performances. In addition, the GBFC finally achieved a 0.56 mW h discharge during 1 hour at 0.5 V without any significant power decrease (Fig. S3, ESI†).

To fully characterize the GBFC stability, the operational stability was investigated by performing constant discharges at 0.6 V each day for one week (Fig. 4D). At day 7, a pseudo power stabilization was observed at 300 μW cm$^{-2}$, corresponding to 40% of the initial power output measured on the first day of use (800 μW cm$^{-2}$).

In parallel, the stability of each bioelectrode was examined periodically through the evolution of OCP of both bioelectrodes over days and the possible leakage of enzymes or NQ in the electrolyte (Fig. S4, ESI†). While negligible leakage of enzymes was observed, a partial leakage of the low soluble NQ redox mediator was recorded by UV-visible experiments. This release corresponds to 20% of the amount of NQ initially entrapped in the MWCNT matrix. Interestingly, while the OCP of the bioanode remains constant at $-0.2$ V, the OCP of the biocathode decreases day after day from 0.59 to 0.46 V, leading to an overall 70 mV decrease of the global OCV of the GBFC. This may directly explain the power decrease observed for the GBFC. The decrease of the catalytic activity at the biocathode could result from a progressive reorientation or disconnection of enzymes within the nanotube compression, leading thus to a decrease in DET efficiency. Another explanation lies in a significant increase of the internal pH due to the enzymatic oxygen reduction. This internal pH shift might inhibit the enzyme activity.

The previously reported mediatorless GBFC, which was limited by the DET of the FAD-GOx, delivered a maximum power density of 1.25 mW cm$^{-2}$, 1.66 mW mL$^{-1}$, 1.85 mW g$^{-1}$ and 0.14 mW h cm$^{-2}$ under continuous discharge in a 50 mM glucose solution. Here we demonstrate that the addition of NQ as a redox mediator increases the power density output to 1.54 mW cm$^{-2}$, 1.92 mW mL$^{-1}$ and 2.67 mW g$^{-1}$. For comparison with recently-developed high power GBFC, a GBFC, described by N. Mano and coworkers, based on bilirubin oxidase and GOx immobilized in CNT–osmium hydrogels, delivered 740 μW cm$^{-2}$ (15 mM glucose).[11] K. Kano and coworkers reported a GBFC in which glucose dehydrogenase, NADH and vitamin K3 were densely entrapped on a carbon-fiber bioanode. This GBFC delivered 1.45 mW cm$^{-2}$ in the presence of 0.4 M glucose.[16]

This novel GBFC configuration is also able to constantly deliver 0.56 mW h cm$^{-2}$ under long-term discharge. Thanks to the involvement of the redox mediator, the GBFC exhibits higher normalized performances in a 4-times reduced volume

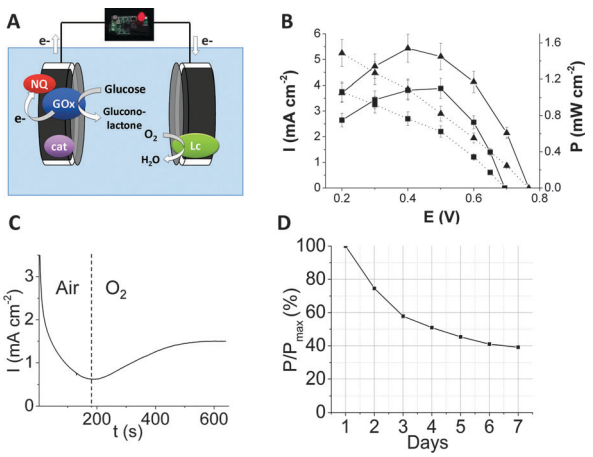


**Fig. 4** (A) Schematic representation of the GBFC (cat is catalase and Lc is laccase); (B) power curves (straight line) and polarization curves (dashed lines) measured by successive 60 s discharge at constant potential. Experiments were conducted in (▲) oxygen saturated buffer and (■) air-saturated buffer (0.2 mol L$^{-1}$ PBS, pH 7, 40 °C); (C) 10 min discharge at 0.6 V under air followed by bubbling of oxygen (0.2 mol L$^{-1}$ PBS, pH 7, 40 °C). (D) Power stability of the GBFC after discharge at 0.6 V performed each day during 7 days. (0.2 mol L$^{-1}$ PBS, pH 7, 25 °C).

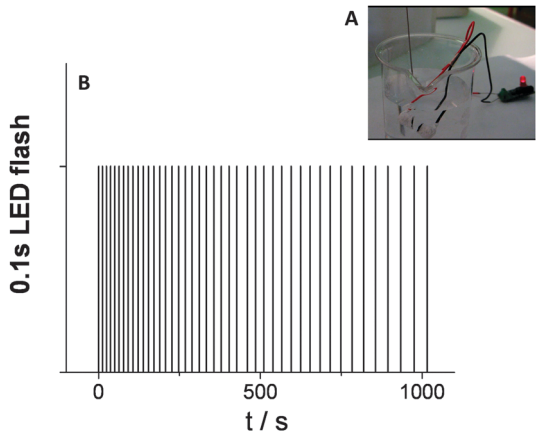


**Fig. 5** (A) Image of the GBFC powering the LED; (B) 0.1 second LED blink over time. The GBFC operates in a quasi-stationary mode in the presence of 50 mM glucose in 0.2 M PBS (pH 7, RT) and a slight oxygen bubbling maintaining the oxygen concentration during the experiment.

(down to 0.16 mL) and with a 10-times reduced weight (down to 90 mg), these dimensions being suitable for surgical insertion into the abdominal cavity of a rat.[5]

To illustrate the high performances of this GBFC, the latter was connected to a LED (Fig. 5). The power management of the GBFC was operated by a low input voltage boost converter (BQ25504, Texas instruments, Dallas, Texas, USA). LED flash of 0.1 s occurs each time the capacitor is fully charged. Fig. 5B shows LED flashes over time for a connected GBFC continuously operating in 50 mM glucose under saturating oxygen conditions. Initially, LED flash occurs every 12 s, while after 20 min of continuous functioning, the charging time to reach the required energy increases to 40 s. Taking into account that a flash consumes 1.13 mW, the GBFC supplies 0.1 mW at the beginning of the experiment and stabilizes its power at 0.03 mW after 20 min.

The video of the experiment is shown in the ESI†.

## Conclusion

In this article, we described the fabrication of a novel bioanode for glucose oxidation. Electrochemical investigations clearly show the advantages of using MET for glucose oxidation with NQ as a redox mediator. Compared to DET, the bioanode achieved 7-fold increase in catalytic current densities, despite the increase in OCP of the bioanode from −0.45 V to −0.2 V. The MWCNT matrix provides a highly conductive and porous material that, in combination with NQ, maximizes the number of wired enzymes. Compared to a mediatorless GBFC, we demonstrate here that the addition of NQ increases the power output density to 1.54 mW $cm^{-2}$, 1.92 mW $mL^{-1}$ and 2.67 mW $g^{-1}$.

These results underline the achievements of a nanoporous bioelectrode in terms of wired enzymes per volume unit while also highlighting the limitations of this kind of electrode materials in terms of substrate permeation. Operational stability shows the exceptional stability of the GBFC under constant discharge, the GBFC being able to deliver 0.56 mW h $cm^{-2}$ under constant discharge at 0.5 V. Also, we demonstrate that these high performances afford the powering of small electronics such as LED devices *via* specific power management.

However, the immobilization of the redox mediator at the bioanode and the optimization of the wiring of laccase at the biocathode are still to be improved to have access to long-term operating GBFC for future supply of long-term implants.

## Acknowledgements

The authors would like thank the Interdisciplinary Energy program of CNRS PR10-1-1 for partial financial support. Hamid Lamraoui is greatly acknowledged for providing specific power management circuit. The Région Rhones-Alpes is acknowledged for the PhD funding of B. Reuillard. The authors are also grateful to the French National Agency for Research (ANR) Emergence-2010 EMMA-043-02, for partial funding.

## Notes and references

1 J. A. Cracknell, K. A. Vincent and F. A. Armstrong, *Chem. Rev.*, 2008, **108**, 2439–2461.
2 I. Willner, Y.-M. Yan, B. Willner and R. Tel-Vered, *Fuel Cells*, 2009, **9**, 7–24.
3 M. J. Cooney, V. Svoboda, C. Lau, G. Martin and S. D. Minteer, *Energy Environ. Sci.*, 2008, **1**, 320–337.
4 S. C. Barton, J. Gallaway and P. Atanassov, *Chem. Rev.*, 2004, **104**, 4867–4886.
5 P. Cinquin, C. Gondran, F. Giroud, S. Mazabrard, A. Pellissier, F. Boucher, J.-P. Alcaraz, K. Gorgy, F. Lenouvel, S. Mathé, P. Porcu and S. Cosnier, *PLoS One*, 2010, **5**, e10476.
6 M. Rasmussen, R. E. Ritzmann, I. Lee, A. J. Pollack and D. Scherson, *J. Am. Chem. Soc.*, 2012, **134**, 1458–1460.
7 A. Szczupak, J. Halámek, L. Halámková, V. Bocharova, L. Alfonta and E. Katz, *Energy Environ. Sci.*, 2012, **5**, 8891–8895.
8 L. Halámková, J. Halámek, V. Bocharova, A. Szczupak, L. Alfonta and E. Katz, *J. Am. Chem. Soc.*, 2012, **134**, 5040–5043.
9 K. MacVittie, J. Halamek, L. Halamkova, M. Southcott, W. D. Jemison, R. Lobel and E. Katz, *Energy Environ. Sci.*, 2013, **6**, 81–86.
10 M. Holzinger, A. Le Goff and S. Cosnier, *Electrochim. Acta*, 2012, **82**, 179–190.
11 F. Gao, L. Viry, M. Maugey, P. Poulin and N. Mano, *Nat. Commun.*, 2010, **1**, 2.
12 A. Zebda, C. Gondran, A. Le Goff, M. Holzinger, P. Cinquin and S. Cosnier, *Nat. Commun.*, 2011, **2**, 370.
13 B. Reuillard, A. Le Goff, C. Agnès, A. Zebda, M. Holzinger and S. Cosnier, *Electrochem. Commun.*, 2012, **20**, 19–22.
14 M. Quan, D. Sanchez, M. F. Wasylkiw and D. K. Smith, *J. Am. Chem. Soc.*, 2007, **129**, 12847–12856.
15 S. Cosnier, M. Stoytcheva, A. Senillou, H. Perrot, R. P. M. Furriel and F. A. Leone, *Anal. Chem.*, 1999, **71**, 3692–3697.
16 H. Sakai, T. Nakagawa, Y. Tokita, T. Hatazawa, T. Ikeda, S. Tsujimura and K. Kano, *Energy Environ. Sci.*, 2009, **2**, 133–138.

 